

## **ANALYSIS OF FREQUENCY SELECTIVE SURFACES FOR RADAR ABSORBING MATERIALS**

**D. Singh<sup>1,\*</sup>, A. Kumar<sup>2</sup>, S. Meena<sup>1</sup>, and V. Agarwala<sup>2</sup>**

<sup>1</sup>Department of Electronics and Computer Engineering, Indian Institute of Technology Roorkee, Uttrakhand-247667, India

<sup>2</sup>Metallurgical and Materials Engineering Department, Indian Institute of Technology Roorkee, Uttrakhand-247667, India

**Abstract**—Nowadays, applications of Frequency Selective Surfaces (FSS) for radar absorbing materials (RAM) are increasing, but it is still a challenge to select a proper FSS for a particular material as well as the dimensions of FSS for optimized absorption. Therefore, in this paper an attempt has been made to optimize the dimensions of FSS for microwave absorbing application using Genetic Algorithm (GA) approach. The considered frequency selective surfaces are composed of conducting patch elements pasted on the ferrite layer. FSS are used for filtration and microwave absorption. In this work, selection and optimization of FSS with radar absorbing material has been done for obtaining the maximum absorption at 8–12 GHz frequency. An equivalent circuit method has been used for the analysis of different FSS, which is further used to design fitness function of GA for optimizing the dimensions of FSS. Eight different available ferrite materials with frequency dependant permittivities and permeabilities have been used as material database. The GA optimization is proposed to select the proper material out of eight available materials with proper dimensions of FSS. The optimized results suggest the material from database and dimensions of FSS. The selected material is then mixed with epoxy and hardener, and coated over the aluminium sheet. Thereafter, all five FSS were fabricated on ferrite coated Al sheets using photolithographic method followed by wet etching. The absorption was measured for all FSS using absorption testing device (ATD) method at X-band. Absorption results showed that significant amount of absorption enhanced with the addition of proper FSS on radar absorbing coating.

---

*Received 16 December 2011, Accepted 17 January 2012, Scheduled 8 February 2012*

\* Corresponding author: Dharmendra Singh (dharmfec@gmail.com).

## 1. INTRODUCTION

Frequency Selective Surfaces (FSS) are planar periodic structures of identical patches or apertures of conducting elements repeating periodically in either a one or two-dimensional array on a dielectric substrate [1–5]. Because of their frequency selective properties, FSS are incorporated in a wide variety of applications such as the realization of reflector antennas, radome design, making polarizers and beam splitters, and also as radar absorbing structure [3, 6–9]. Radar Absorbing Materials (RAM) with FSS can improve absorption characteristic as it has combined characteristics of FSS as well as RAM. The frequency behavior of the FSS depends on the shape of the elements (apertures/patches), their size and spacing, and thickness of the metal screen. Generally FSS are employed in front of a grounded dielectric slab (substrate) to synthesize high-impedance absorbing surfaces [3–6, 10, 11].

Incident power absorbed by this type of absorbers generally relies on two aspects: one is by resistive patches (i.e., FSS) and second is due to the presence of radar absorbing materials. Compared with traditional RAM coatings, FSS with RAMs have been demonstrated to be lighter, thinner and broadband [2]. However, FSS type RAM's absorbing properties are affected by many parameters, such as patch type, pattern and size, periodicity, and RAM layer's electromagnetic parameters, thickness, etc. Therefore, different FSS shows different response for a particular radar absorbing material. So, it becomes necessary to investigate the effect of implementing FSS on RAM.

Implementation of FSS on ferrite reduces the thickness of absorber as well as increases the absorption and its physical strength, which is more favorable for practical applications, but still selection of FSS for a particular RAM is quite challenging. Therefore, there is a need to develop such a technique by which FSS and material selection can be done. For this purpose, FSS and material were optimized through genetic algorithm approach. The equivalent transmission line method was used to identify best ferrite material, optimization of RAM thickness and optimization of different FSS parameters.

This paper is divided into six sections. Section 2 gives brief details of FSS analysis. Section 3 defines methodology which includes optimization of FSS on RAM. Implementation of FSS on RAM coating is discussed in Section 4. Experimental setup for absorption testing is discussed in Section 5. Results and discussion are given in Section 6, followed by conclusion in Section 7.

## 2. THEORETICAL ANALYSIS OF FSS

FSS are planar periodic structures that behave like filters to electromagnetic energy. The available results in literature show that FSS can modify and improve the absorbing performances of RAM [3]. Many materials have been developed for RAM application. In this paper, an attempt has been made to combine FSS with RAM. Different elemental shapes of FSS offer different frequency responses. Factors influencing FSS response are:

1. FSS's element geometry,
2. Conductivity of FSS's material,
3. Dielectric substrate to support FSS and
4. Incidence angle of the signal.

When electromagnetic energy is incident on a FSS, currents are induced on the conducting elements. These induced currents then re-radiate EM waves from these conducting elements. Various methods for analyzing periodic structures have been developed with computational intensive approaches such as the mutual impedance method [1], the method of moments (MoM) [12], the finite element method (FEM) [13], the finite-difference time-domain (FDTD) method [4], and Equivalent Circuit (EC) method [4, 14–17]. Out of these, EC method was chosen as it is a simple and powerful technique. Using this technique, FSS can be modeled as energy-storing inductive or capacitive components which are determined by the shape of its elements, but the analysis is limited to linear polarizations and simple FSS element geometries [17].

The configuration of each element (either patch or aperture within an array of periodic cells), as well as the vertical and horizontal spacings, will contribute to the form of the scattered fields-transmitted or reflected [29]. The basic rule of design is to make the loop

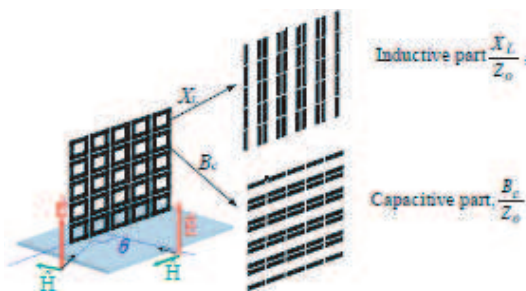


**Figure 1.** The equivalent circuit approximation of the square loop FSS [17].

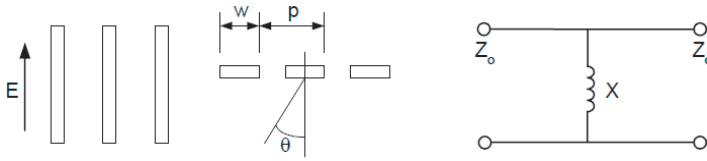


**Figure 2.** Equivalent circuit parameters for TE incidence on the plane  $T$  [18].

circumference approximately equal to the wavelength of resonant frequency. The period of repeating elements should be less than the shortest wavelength considered in the operating band for zero degree signal incidence to suppress the grating lobes. For larger incidence angle, spacing should be kept less than one-half of the wavelength [30]. However, this is just to determine the starting value for designing FSS. The final element dimensions need to be fine-tuned to meet the desired frequency response. Analysis technique can be explained easily using the example of single loop (SL) FSS. For SL-FSS, resonance occurs when each half loop acts as a dipole [18, 19]. The square loops are separated into vertical and horizontal conducting strips, and can be modeled as inductive and capacitive components respectively as shown in Figure 1 for TE-wave, which has the electric field parallel to the vertical strips. The vertical strips can be modeled as a shunt inductive reactance in the EC circuit.

For an array of thin, continuous, infinitely long and perfectly conducting narrow strips, the shunt impedance is either inductive or capacitive, depending on the incident wave, whether it is polarized parallel to or perpendicular to edge of the strips. For problem formulation, an array of metal strip with zero thickness, width ' $w$ ' and period ' $p$ ' as shown in Figure 2 was considered. The TE plane wave makes an angle  $\theta$  onto the strip [18].

The equivalent circuit inductive reactance for the electric vector parallel to the conductor (normalized free space impedance) is given by [14, 18]

$$\frac{X(w)}{Z_0} = F(p, w, \lambda) = \frac{p}{\lambda} \cos\theta \left[ \ln \left( \operatorname{cosec} \left( \frac{\pi w}{2p} \right) \right) + G(p, w, \lambda, \theta) \right] \quad (1)$$

where,  $G(p, w, \lambda, \theta) = \frac{(1-\beta^2)^2 [(1-\frac{\beta^4}{4})(A_1+A_2)+4\beta^2 A_1 A_2]}{2[(1-\frac{\beta^2}{4})+\beta^2(1+\frac{\beta^2}{2}-\frac{\beta^4}{8})(A_1+A_2)+2\beta^6 A_1 A_2]}$ ,  $A_{1,2} = \frac{1}{\sqrt{1 \pm \frac{2p \sin \theta}{\lambda} - (\frac{p \cos \theta}{\lambda})^2}} - 1$ , and  $\beta = \sin \frac{\pi w}{2p}$ , where,  $\lambda$  is the wavelength and  $Z_0$  is the characteristic impedance of free space. Similarly, the incident magnetic field vector is parallel to the metal strips, having a

period ‘ $p$ ’, and a gap spacing ‘ $g$ ’ (the electric vector perpendicular to the conductor has capacitive susceptance), and is incident at an angle of ‘ $\theta$ ’, as shown in Figure 3 [18].

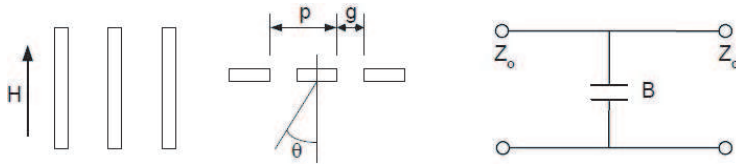


**Figure 3.** Equivalent circuit parameters for TM incidence on the plane  $T$  [18].

**Table 1.** Equivalent circuit diagram for different FSS.

S. No	FSS	Circuit	Equivalent Circuit	Equivalent Inductance	Equivalent Capacitance	Reference
1	Single Square Loop			$\frac{X_L}{Z_0} = \frac{d}{p} F(p, 2s, \lambda)$	$\frac{B_C}{Z_0} = 4 \frac{d}{p} F(p, g, \lambda)$	[14, 16, 17]
2	Double Square Loop			$\left(\frac{X_L}{Z_0}\right)_1 = F(p, s_1, \lambda)$ $\left(\frac{X_L}{Z_0}\right)_2 = F(p, s_2, \lambda)$	$\left(\frac{B_C}{Z_0}\right)_1 = 4F(p, g_1, \lambda)$ $\left(\frac{B_C}{Z_0}\right)_2 = 4F(p, g_2, \lambda)$	[16, 21, 32]
3	Triple Square Loop			$\left(\frac{X_L}{Z_0}\right)_1 = F(p, s_1, \lambda)$ $\left(\frac{X_L}{Z_0}\right)_2 = F(p, s_2, \lambda)$ $\left(\frac{X_L}{Z_0}\right)_3 = F(p, s_3, \lambda)$	$\left(\frac{B_C}{Z_0}\right)_1 = 4F(p, g_1, \lambda)$ $\left(\frac{B_C}{Z_0}\right)_2 = 4F(p, g_2, \lambda)$ $\left(\frac{B_C}{Z_0}\right)_3 = 4F(p, g_3, \lambda)$	[16, 20]
4	Cross Dipole			$\frac{X_L}{Z_0} = \frac{d}{p} F(p, w, \lambda)$	$B_s = 4 \frac{w}{p} F(p, g, \lambda)$ $B_d = 4 \frac{d}{p} F(p, p-w, \lambda)$	[16, 20, 22]
5	Jerusalem Cross Array			$\frac{X_L}{Z_0} = \left(\frac{d}{p}\right) F(p, w, \lambda)$	$B_d = 4 \frac{(2h+g)}{p} F(p, p-d, \lambda)$ $B_s = 4 \frac{d}{p} F(p, g, \lambda)$	[16, 20, 23]

Note: All necessary parameter defining FSS are shown in the table.

The capacitive susceptance (normalized free space admittance) is calculated by

$$\frac{B(g)}{Z_0} = 4F(p, g, \lambda) \quad (2)$$

where, 'g' is the gap between the conductor and  $F$  is function of  $p$ ,  $g$  and  $\lambda$ , which is obtained by replacing 'w' by 'g' in Eq. (1). The equations presented above are valid for wavelengths and angles of incidence  $\theta$  in the range  $p(1 + \sin \theta)/\lambda < 1$  and assume that  $w \ll p < \lambda$  and  $g \ll p$  [18] and are valid for plane wave incident in the  $E$  or  $H$  plane only. The equivalent impedance of the SL FSS is given by

$$Z_{\text{fss}} = j \left( X_L - \frac{1}{B_C} \right) \quad (3)$$

The various FSS structures are considered in the present study, and their equivalent circuits are given in Table 1.

## 2.1. Selection of Substrate for FSS

Generally, dielectric substrates are used to provide structural support and stabilization to the angular response of FSS [22, 23]. The dielectric substrate's permittivity has a great influence on FSS design. In a single layer of FSS, FSS is attached to one side of the dielectric substrate. The resonant frequency ( $f_r$ ) of FSS array is dependent on the thickness of the supporting dielectric substrate. If the FSS is loaded with thick dielectrics, the resonance frequency is reduced by a factor  $\sqrt{\epsilon_{\text{eff}}}$  [1, 31]. Different FSS/dielectric arrangements will influence the frequency selective response to a different extent and improve the stability of FSS performance over a range of incident angles. In other words, with the use of dielectrics, FSS can be made less sensitive to incident angles.

In the present study, ferrite coated Al sheet was used instead of dielectric substrate. Ferrites in general are the magnetic oxides of iron containing magnetic dipoles arranged in a manner which produces spontaneous magnetization while maintaining good dielectric properties, therefore, it can be used as a base material to implement FSS. The electromagnetic energy is dissipated in a ferrite majorly due to magnetic effect. The loss mechanism in ferrite material depends on the interaction between magnetic vector of electromagnetic wave and the magnetization of the ferrites. In an un-magnetized ferrite the magnetic dipoles are randomly distributed and as a magnetic field is applied, the magnetic dipoles orientation changes according to type of ferrite.

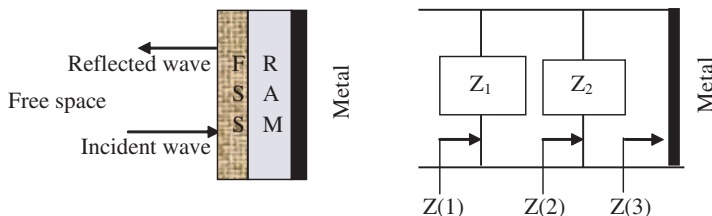


**Figure 4.** Geometry of the FSS impregnated ferrite absorber and equivalent transmission line model.

### 2.2. Implementation of FSS on RAM

Frequency selective patches were impregnated on a ferrite material backed with Al plate as shown in Figure 4. The EM wave impedance of the perfect electric conductor is zero.  $Z(2)$  is the effective impedance at the interface of RAM coating and FSS, and  $Z(1)$  is the overall effective impedance of FSS and RAM [5, 24, 27].

The reflection coefficient of the FSS impregnated ferrite absorber is given by

$$R = \frac{Z(1) - Z_0}{Z(1) + Z_0} \tag{4}$$

$$\text{Absorption (in dB)} = -20 \log_{10} |R| \tag{5}$$

The impedance after RAM coating on the conductor plate will be given by

$$Z(2) = Z_2 \frac{Z(3) - jZ_2 \tan(\theta_2)}{Z_2 - jZ(3) \tan(\theta_2)} \tag{6}$$

The impedance due to perfect metal conductor will be zero, so  $Z(3) = 0$

$$Z(2) = -jZ_2 \tan(\theta_2) \tag{7}$$

where,  $Z_2$  is the characteristic impedance of the Radar Absorbing Material (coating)

$$\theta_2 = K_2 d \sqrt{1 - \left(\frac{K_0}{K_2}\right)^2 \sin^2 \theta_0} \quad \text{and}$$

$$K_2 = \omega \sqrt{\mu_2 \varepsilon_2}, \quad K_0 = \omega \sqrt{\mu_0 \varepsilon_0}$$

where,  $\theta_0$  is the angle of incidence,  $d$  the thickness of the ferrite layer,  $\varepsilon_0$ , and  $\varepsilon_2$  and  $\mu_0$ ,  $\mu_2$  the permittivities and permeabilities of free space and ferrite material respectively.  $Z(2)$  is the effective impedance at the

interface of RAM coating and FSS. Thus impedance at the interface of free space and FSS is

$$Z(1) = \frac{Z(2) * Z_1}{Z(2) + Z_1} \quad (8)$$

where,  $Z_1$  is the effective impedance of the FSS structure selected and can be obtained using equivalent impedance as given in Eq. (3) for the case of single square loop FSS. The equivalent inductance and capacitance for equivalent circuit which were used for optimization are given in Table 1. These equivalent inductance and capacitance are further utilized to find  $Z_{\text{fss}}$  as Eq. (3) by which the calculation of reflection loss can be computed using Eqs. (4) and (5).

### 3. METHODOLOGY: OPTIMIZATION OF FSS ON RAM

There are many physical parameters needed to be determined, such as proper ferrite material (i.e., proper permittivity, permeability) and thickness of ferrite coating as well as shape (i.e., periodicity, gap and width) of FSS structure (which defines inductance and capacitance of the structure by which resultant impedance can be calculated). GA was used as an optimization technique to optimize the various parameters such as periodicity ' $p$ ', gap ' $g$ ', width ' $s$ ', ferrite material ' $m$ ' and thickness of ferrite coating ' $t$ ', as GA is very powerful for problems that have a large number of variables [28]. All dimensions considered are in meter. Frequency selective surfaces for the radar absorbing material were designed for single layer RAM coating with FSS impregnated on it. To replicate mathematically the FSS for RAM, the transmission line equivalent method as discussed in Subsection 2.2 was used. Five different FSS as shown in Table 1 were critically analyzed for the absorption purpose at X-band. The eight types of ferrite material (details given in Table 2) were used for optimization. The corresponding permittivity and permeability of these materials at different frequencies are listed in Table 2. According to change in the value of  $\alpha$  and  $\beta$ ,  $\mu$  and  $\varepsilon$  may be computed for different frequencies at X-band [25, 30].

So, it is important to select proper material from database with suitable FSS for better absorption at X-band. Therefore, for this purpose GA optimization has been used and details are given in Figure 5(a).

### 4. IMPLEMENTATION OF FREQUENCY SELECTIVE SURFACES ON RAM COATING

The genetic algorithm is an iterative optimization procedure that starts with a randomly selected population of potential solution and generally evolve towards better solutions through the application of genetic operator. Their repetitive applications to the population of potential solutions result in an optimization process that resembles natural evolution. The three genetic operator governing the iterative search are often referred to as the selection, cross-over and mutation operators. The probabilistic nature of all the three operators greatly enhance the capabilities of the algorithm to search for a global rather than local fitness function. The flow chart of GA optimization technique is shown in Figure 5(b). The Fitness function for optimizing Eq. (5) with

**Table 2.** Material database used for optimization [25].

S No	$\epsilon_r(f) = \frac{\epsilon_r(8GHz)}{f^\alpha}$ , $\epsilon_i(f) = \frac{\epsilon_i(8GHz)}{f^\beta}$ , $\mu_r(f) = \frac{\mu_r(8GHz)}{f^\alpha}$ , $\mu_i(f) = \frac{\mu_i(8GHz)}{f^\beta}$				
	Material	$\epsilon_r(8GHz)$ $\alpha$	$\epsilon_i(8GHz)$ $\beta$	$\mu_r(8GHz)$ $\alpha$	$\mu_i(8GHz)$ $\beta$
1	Ba(MnTi) <sub>1.7</sub> Fe <sub>8.6</sub> O <sub>19</sub>	5.63 0.019252	2.41 0.049792	0.12 -0.08951	2.5 0.036445
2	Ba(MnTi) <sub>1.8</sub> Fe <sub>8.4</sub> O <sub>19</sub>	2.99 -0.01396	3.24 0.045507	1.73 0.021888	0.2 -0.08288
3	Ba(MnTi) <sub>1.9</sub> Fe <sub>8.2</sub> O <sub>19</sub>	3.99 -0.00243	1.84 0.02929	1.14 -0.01273	1.26 0.002088
4	SrZn <sub>1.2</sub> Fe <sub>13.2</sub> Sn <sub>0.6</sub> Mn <sub>0.6</sub> O <sub>23.8</sub>	2.67 -0.02174	0.7 0.00585	0.091 -0.08504	1.795 0.004794
5	BaTiO <sub>3</sub>	3.325 -0.00369	13.65 0.059571	1 0	0 0
6	Ba(MnTi) <sub>3.5</sub> Fe <sub>5.0</sub> O <sub>19</sub>	6.485 0.022805	3.816 0.056184	1.893 0.027582	0.04 -0.13677
7	Ba(MnTi) <sub>1.6</sub> Fe <sub>8.8</sub> O <sub>19</sub>	7.08 0.036194	0.36 0.03738	1.92 0.022261	1.15 0.02103
8	Ba(Mn <sub>0.15</sub> Co <sub>0.85</sub> ) <sub>2</sub> Fe <sub>16</sub> O <sub>27</sub>	8.837 0.010656	1.84 0.00826	0.745 0.009302	2.015 0.020206

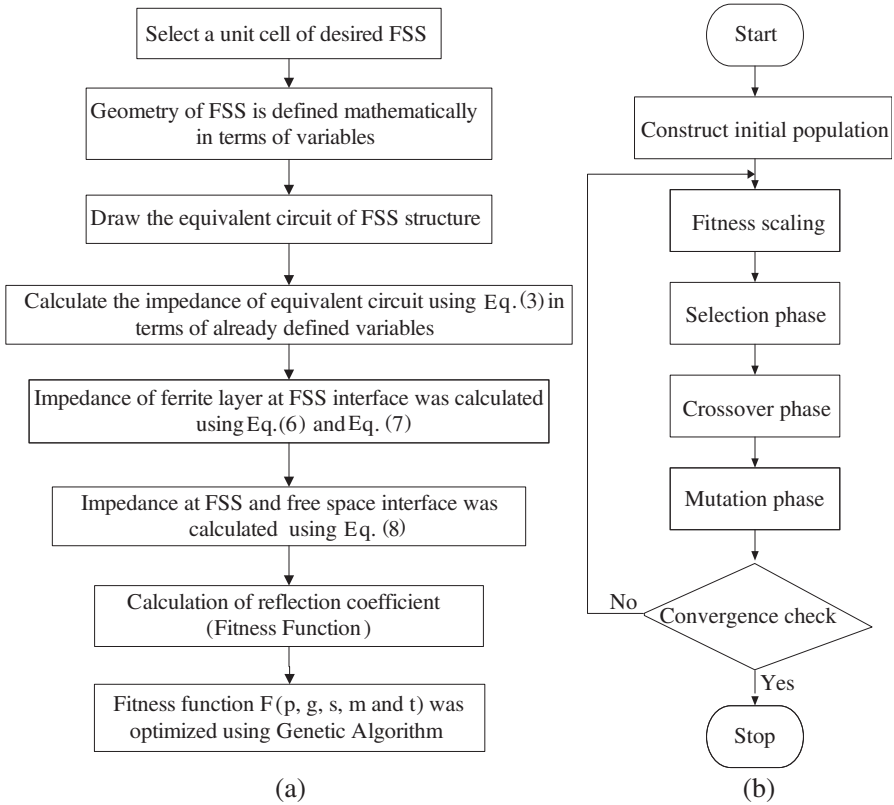


**Figure 5.** Steps used before optimization to FSS on RAM (a) and flow chart of genetic algorithm (b).

different equations as shown in column 3 and 4 of Table 1 were used and the fitness function was optimized using “gatool” of MATLAB with different parameters. The optimized results for single square loop FSS i.e., gap between patches ‘ $g$ ’, width of patch ‘ $s$ ’, length of the patch ‘ $d$ ’, material ‘ $m$ ’ ( $\text{Ba}(\text{MnTi})_{1.6}\text{Fe}_{8.8}\text{O}_{19}$ ) and the thickness of ferrite coating ‘ $t$ ’ are shown in Table 3. Period ‘ $p$ ’ depends on the values of ‘ $g$ ’ and ‘ $d$ ’, hence it is not shown. In the same way variables for other FSS are also shown; not shown variables can be inferred from shown variables. Double square and triple square loop FSS being more complex geometry require more parameters to define geometry.

For simplicity and comparison of all FSS, all Al sheets were coated with the material  $\text{Ba}(\text{MnTi})_{1.6}\text{Fe}_{8.8}\text{O}_{19}$  for 0.2 mm thickness, as it was not possible to spray coat Al sheets for the dimension optimized through GA. The ferrite coating was dried for more than 8–10 h. A thin

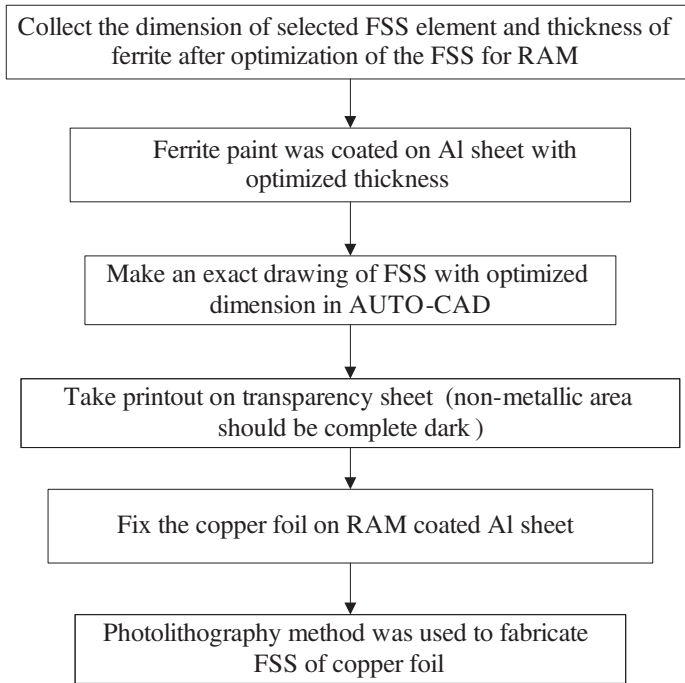


**Figure 6.** Flow chart to fabricate FSS on RAM.

copper foil was stacked on RAM coated Al sheet by applying a very thin layer of epoxy based adhesive (Araldite) between both surfaces (i.e., copper foil and RAM coated Al sheet) and then a pressure was applied, by which adhesive layer thickness becomes nearly zero. The details of fabrication are given in flow chart shown in Figure 6. The complete structure had been then dried for 48 h.

## 5. EXPERIMENTAL SETUP

The absorption properties of designed FSS have been measured by ingeniously developed Absorption Testing Device (ATD) at 8–12 GHz. Details are shown in Figure 7 [26]. A 2 mm thick  $94.5 \times 74.2 \text{ mm}^2$  Al sheet was used for coating ferrite material and fabricating FSS on it, which was used in ATD for absorption testing. In order to measure absorption from ATD, power reflected from coated sample was subtracted from power reflected from uncoated sample.

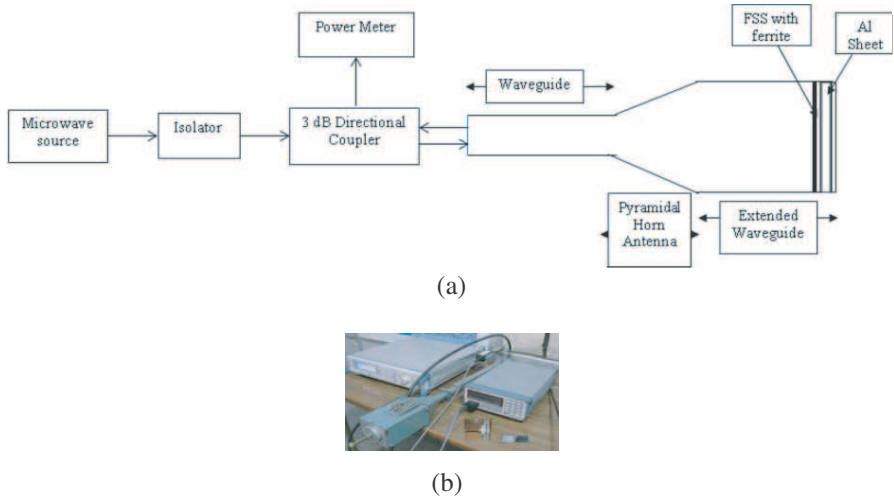


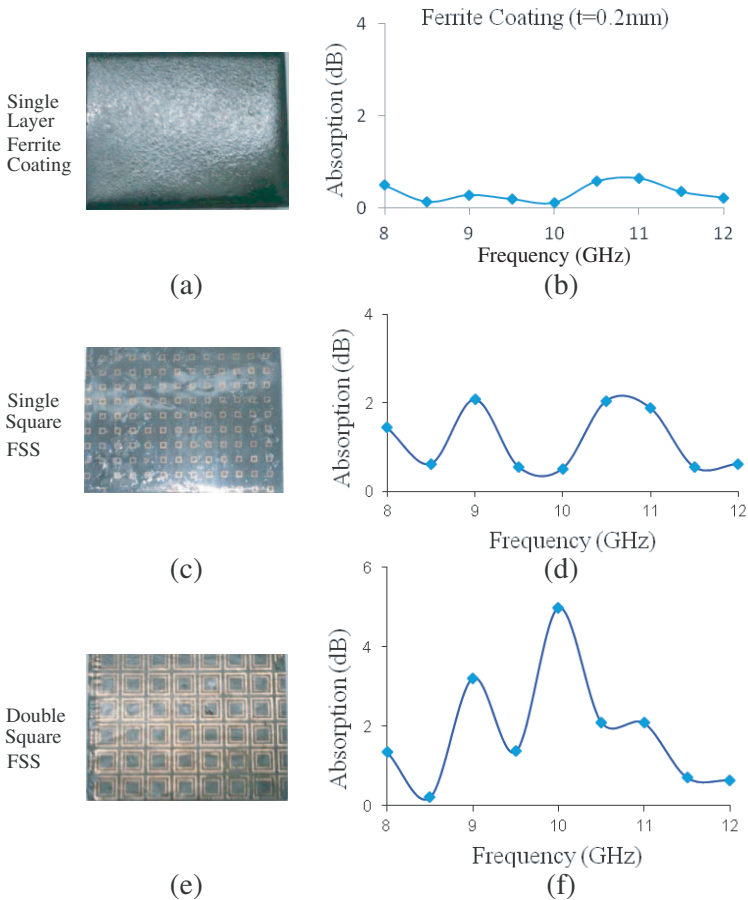
**Figure 7.** (a) Schematic diagram of Absorption Testing Device (ATD) and (b) experimental setup for absorption measurement.

**Table 3.** Optimized results for different FSS.

S No	FSS	Optimized Dimension (in meter)								
		g	s	d	m	t				
1	Single Square loop	g	s	d	m	t				
		0.00427	0.00054	0.00181	7	0.00039				
2	Double Square loop	g <sub>1</sub>	g <sub>2</sub>	s <sub>1</sub>	s <sub>2</sub>	d <sub>2</sub>	m	t		
		0.00142	0.0010	0.00051	0.00098	0.00609	7	0.00040		
3	Triple Square loop	g <sub>1</sub>	g <sub>2</sub>	g <sub>3</sub>	s <sub>1</sub>	s <sub>2</sub>	s <sub>3</sub>	d <sub>2</sub>	m	t
		0.00182	0.00127	0.00160	0.00169	0.00193	0.00072	0.00864	7	0.00039
4	Cross Dipole	g	w	d	m	t				
		0.00956	0.00782	0.01470	7	0.00047				
5	Jerusalem cross	g	w	d	h	p	m	t		
		0.00473	0.00286	0.00848	0.00044	0.01336	7	0.00043		

### 6. RESULTS AND DISCUSSION

The objective of this paper was to select a ferrite material out of available ferrite materials and to determine the FSS with various parameters, such as periodicity, gap, and width. The implementation has been done as discussed in Section 4, and the results of optimization are shown in Table 3. Absorption characteristics of ferrite coating, with and without FSS (as considered in Table 1) were checked using Attenuation Testing Device (ATD). Firstly, Al sheet was coated with  $Ba(MnTi)_{1.6}Fe_{8.8}O_{19}$  (material No. 7 Table 2 as obtained from optimized results) as shown in Figure 8(a) and its ATD result is shown in Figure 8(b). It is observed from Figure 8(b) that the ferrite coated Al sheet has maximum absorption of 0.58 dB at 10.5 and 11 GHz.



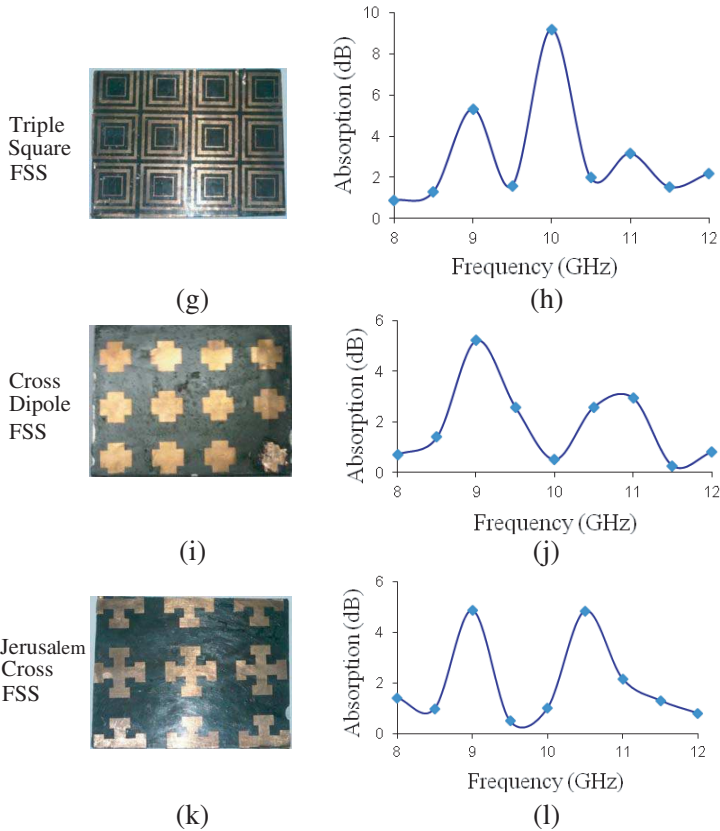


**Figure 8.** Effect of different FSS on microwave absorption on normal incidence.

After that a single square FSS was fabricated over  $\text{Ba}(\text{MnTi})_{1.6}\text{Fe}_{8.8}\text{O}_{19}$  ferrite, as shown in Figure 8(c). In this graph, maximum 2 dB absorption was observed at 9 GHz and 10.5 GHz, as shown in Figure 8(d). The enhancement in absorption may be due to the interaction between microwave with conducting copper and ferrite material which may lead to more internal reflections [29].

In another ferrite coated Al sheet, a double square FSS (as given in Table 1, serial No. 2) was fabricated, which is shown in Figure 8(e). Figure 8(f) shows corresponding absorption behavior and in this case maximum 4.99 dB absorption was observed at 10 GHz frequency.

Figure 8(g) shows triple square FSS (as shown in Table 1, serial No. 3), and corresponding absorption behavior is shown in Figure 8(h).

A maximum absorption of 9.19 dB at 10 GHz was observed.

Figures 8(i) and (k) show Cross Dipole and Jerusalem FSS respectively (as shown in Table 1, serial Nos. 4 and 5) and corresponding absorption behavior are shown in Figures 8(j) and (l). It was observed that the maximum absorption in case of Cross Dipole FSS was 5.22 dB at 9 GHz and a maximum absorption of 4.86 dB at 9 GHz & 10.5 GHz in case of Jerusalem Cross FSS was observed.

The results shown in Figures 8(b), (d), (f), (h), (j) and (l) suggest that the implementation of different FSS on ferrite coated Al sheet increases the absorption amount. The maximum absorption was observed in case of triple square FSS in comparison to the other considered FSS. It can be inferred that the amount of absorption will be enhanced significantly with the use of triple square FSS without changing the thickness of the coating at selected X-band.

## 7. CONCLUSION

The dimensions of the perfect conducting FSS, and RAM's thickness were optimized using genetic algorithm. The structure prepared in this work presents proper characteristics for handling, flexibility and lightweight, meeting requirements for its application. Another important advantage of the processed FSS on RAM is its low specific mass compared to single ferrite coating.

The ferrite paint was coated on an Al sheet, and the FSS was implemented on it with optimized dimensions and then tested using ATD (X-band). It has been observed from ATD testing that maximum attenuation was found in case of triple square frequency selective surfaces. Implementation of FSS on coated Al sheet has shown encouraging results. The results show the enhancement in absorption with the addition of FSS on RAM. This type of analysis helps in reducing thickness of the radar absorbers and in selecting proper FSS and RAM for the given application.

## REFERENCES

1. Munk, B. A., *Frequency Selective Surfaces — Theory and Design*, John Wiley and Sons, Inc., New York, 2000.
2. Wu, T. K., *Frequency Selective Surfaces and Grid Array*, John Wiley and Sons, Inc., New York, 1995.
3. Liu, H. T., H. F. Cheng, Z. Y. Chu, et al., "Absorbing properties of frequency selective surface absorbers with cross-shaped resistive patches," *Material Design*, Vol. 28, 2166–2171, 2007.

4. Mias, C., C. Tsakonas, and C. Oswald, "An investigation into the feasibility of designing frequency selective windows employing periodic structures, (Ref. AY3922)," Tech. Rep., Final Report for the Radio-communications Agency, Nottingham Trent University, 2001.
5. Sakran, F. and Y. Neve-Oz, "Absorbing frequency-selective-surface for the mm-wave range," *IEEE Transactions on Antennas and Propagation*, Vol. 56, No. 8, 2649–2655, 2008.
6. Arya, F., M. Matthew, H. Christian, and V. Rüdiger, "Efficient procedures for the optimization of frequency selective surfaces," *IEEE Transactions on Antennas and Propagation*, Vol. 56, No. 5, 1340–1349, 2008.
7. Munk, B. A., R. J. Luebbers, and R. D. Fulton, "Transmission through a two-layer array of loaded slots," *IEEE Transactions on Antennas and Propagation*, Vol. 22, 804–809, 1974.
8. Ulrich, R., "Far-infrared properties of metallic mesh and its complementary structure," *Infrared Physics*, Vol. 7, 37–55, 1967.
9. Durschlag, M. S. and T. A. DeTemple, "Far-IR optical properties of freestanding and dielectrically backed metal meshes," *Applied Optics*, Vol. 20, 1245–1253, 1981.
10. Chen, H. Y., X. Y. Hou, and L. J. Deng, "A novel microwave absorbing structure using FSS metamaterial," *PIERS Proceedings*, 1195–1198, Moscow, Russia, Aug. 18–21, 2009.
11. Simms, S. and V. Fusco, "Tunable thin radar absorber using artificial magnetic ground plane with variable backplane," *Electronics Letters*, Vol. 42, No. 21, 1197–1198, 2006.
12. Kominami, M., H. Wakabayashi, S. Sawa, and H. Nakashima, "Scattering from a periodic array of arbitrary shaped elements on a semi infinite substrate," *Electronics and Communications in Japan (Part I: Communications)*, Vol. 77, No. 1, 85–94, 1994.
13. Bardi, I., R. Remski, D. Perry, and Z. Cendes, "Plane wave scattering from frequency-selective surfaces by the finite-element method," *IEEE Transactions on Magnetics*, Vol. 38, No. 2, 641–644, 2002.
14. Langley, R. J. and E. A. Parker, "Equivalent circuit model for arrays of square loops," *Electronic Letters*, Vol. 18, No. 7, 294–296, 1982.
15. Lee, C. K. and R. J. Langley, "Equivalent-circuit models for frequency-selective surfaces at oblique angles of incidence," *IEE Proceeding H*, Vol. 132, No. 6, 395–399, 1985.
16. Dubrovka, R., J. Vazquez, C. Parini, and D. Moore, "Equivalent

- circuit method for analysis and synthesis of frequency selective surfaces,” *IEE Proceeding on Microwave Antennas Propagation*, Vol. 153, No. 3, 213–220, 2006.
17. Sung, G. H., K. W. Sowerby, and A. G. Williamson, “Equivalent circuit modelling of a frequency selective plasterboard wall,” *IEEE Antennas and Propagation Society International Symposium*, Vol. 4A, 400–403, 2005.
  18. Philippakis, M., C. Martel, D. Kemp, S. Appleton, and S. Massey, “Application of FSS structures to selectively control the propagation of signals into and out of buildings annex 3: Enhancing propagation into buildings,” Final Report, ERA Project 51-CC-12033, ERA Report, 2004.
  19. Campos, A. L. P. D. S., “Analysis of frequency selective surfaces with metallic and dielectric losses at millimeter wave range,” *Int. J. Infrared Milli Waves*, Vol. 29, 684–692, 2009.
  20. Kumar, R., “Study and characterization of Zn-Mn and Zn-Co ferrite using FSSs at microwave frequency”, ME Dissertation in Electronics and Communication Engineering, Department of E. & C., IIT Roorkee, Mar. 1998.
  21. Langley, R. J. and E. A. Parker, “Double-square frequency-selective surfaces and their equivalent circuit,” *Electronics Letters*, Vol. 19, No. 17, 675–677, 1983.
  22. Kiani, G. I., A. R. Weily, and K. P. Esselle, “Frequency selective surface absorber using resistive cross-dipoles,” *IEEE Antennas and Propagation Society International Symposium*, 4199–4202, 2006.
  23. Langley, R. J. and A. J. Drinkwater, “Improved empirical model for the jerusalem cross,” *Microwaves, Optics and Antennas, IEE Proceedings H*, Vol.129, No. 1, 1–6, 1982.
  24. Huiling, Z., G. B. Wan, and W. Wan, “Absorbing properties of frequency selective surface absorbers on a lossy dielectric slab,” *PIERS Proceedings*, 165–168, Beijing, China, Mar. 23–27, 2009.
  25. Parida, R. C., D. Singh, and N. K. Agarwal, “Implementation of multilayer ferrite radar absorbing coating with genetic algorithm for radar cross-section reduction at X-band,” *Indian Journal of Radio & Space Physics*, Vol. 36, No. 2, 145–152, 2007.
  26. Meshram, M. R., N. K. Agrawal, B. Sinha, and P. S. Misra, “A study on the behaviour of M-type barium hexagonal ferrite based microwave absorbing paints,” *Bulletin of Materials Science*, Vol. 25, No. 2, 169–173, 2002.
  27. Park, K. Y., S. E. Lee, C. G. Kim, and J. H. Han, “Fabrication and

- electromagnetic characteristics of electromagnetic wave absorbing sandwich structures,” *Composites Science and Technology*, Vol. 66, 576–584, 2006.
28. Kern, D. J. and D. H. Werner, “A genetic algorithm approach to the design of ultra-thin electromagnetic bandgap absorbers,” *Microwave and Optical Technology Letters*, Vol. 38, No. 1, 61–64, 2003.
  29. Folgueras, L. d. C., E. L. Nohara, R. Faez, and M. C. Rezende, “Dielectric microwave absorbing material processed by impregnation of carbon fiber fabric with polyaniline,” *Materials Research*, Vol. 10, No. 1, 95–99, 2007.
  30. Sugimoto, S., S. Kondo, K. Okayama, H. Nakamura, D. Book, T. Kagotani, and M. Homma, “M-type ferrite composite as a microwave absorber with wide bandwidth in GHz,” *IEEE Transactions on Magnetism*, Vol. 35, No. 5, 3154–3156, 1999.
  31. Filippo, C., A. Claudio, M. Agostino, and E. Prati, “Waveguide dielectric permittivity measurement technique based on resonant FSS filters,” *IEEE Microwave and Wireless Components Letters*, Vol. 21, No. 5, 273–275, 2011.
  32. Luo, X. F., P. T. Teo, A. Qing, and C. K. Lee, “Design of double-square-loop frequency-selective surfaces using differential evolution strategy coupled with equivalent-circuit model,” *Microwave and Optical Technology Letters*, Vol. 44, No. 2, 159–162, 2005.